Communication

Solid-State NMR Fermi Contact and Dipolar Shifts in Organometallic Complexes and Metalloporphyrins

Yong Zhang, Haihong Sun, and Eric Oldfield

J. Am. Chem. Soc., **2005**, 127 (11), 3652-3653• DOI: 10.1021/ja043461j • Publication Date (Web): 24 February 2005

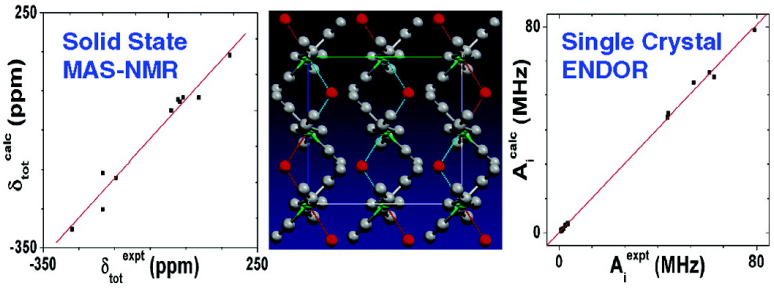

More About This Article

Additional resources and features associated with this article are available within the HTML version:

- Supporting Information
- Links to the 10 articles that cite this article, as of the time of this article download
- Access to high resolution figures
- Links to articles and content related to this article
- Copyright permission to reproduce figures and/or text from this article

View the Full Text HTML

J|A|C|S
COMMUNICATIONS

Published on Web 02/24/2005

Solid-State NMR Fermi Contact and Dipolar Shifts in Organometallic Complexes and Metalloporphyrins

Yong Zhang, Haihong Sun, and Eric Oldfield*

Departments of Chemistry and Biophysics, University of Illinois at Urbana-Champaign, 600 South Mathews Avenue, Urbana, Illinois 61801

Received October 28, 2004; E-mail: eo@chad.scs.uiuc.edu

The NMR spectral shifts of paramagnetic metal complexes can provide valuable information about structure and bonding.[1] These shifts are made up of both isotropic Fermi contact and anisotropic dipolar hyperfine interactions, which, especially at low temperatures, can be very large, on the order of 1 MHz. In early work, Kreilick et al. investigated Cu^{II}(DL-alanine)$_2$·H_2O (**1**) single crystals using ^{1}H NMR and reported both isotropic and anisotropic hyperfine interactions and used these to determine the relative positions of nuclei in the ligands with respect to the central metal.[2,3] This approach also enabled assignments for AgTPP (**2**, TPP = *meso*-tetraphenylporphyrin), which were found to be in close agreement with single-crystal ENDOR results.[4] The ENDOR hyperfine parameters for CuTPP (**3**) were also reported[4] and confirmed in later studies.[5] More recently, another approach, "magic-angle" sample spinning (MAS) NMR, has been used to investigate a variety of paramagnetic solids, including Cu(DL-ala)$_2$·H_2O and V(acac)$_3$ (**4**, acac = $CH_3COCHCOCH_3$), and both ^{13}C and ^{1}H/^{2}H shifts have been reported.[6,7] Surprisingly, however, there have been no reports of the calculation of these NMR Fermi contact and dipolar interactions using quantum chemical methods, although there have been reports of the successful evaluation of large (up to ~6000 ppm) hyperfine shifts in solution NMR spectra of proteins and model systems.[8,9]

In this communication, we present the results of the first quantum chemical investigations of the solid-state MAS NMR and single-crystal NMR of a variety of paramagnetic solids, together with an investigation of several ENDOR spectra.

We used the hybrid Hartree−Fock density functional theory (HF-DFT) method B3LYP[10] in our calculations, together with a large basis set,[11] used previously to evaluate solution NMR hyperfine shifts as well as ESR properties.[9,12] X-ray crystal structures[13] of **2**−**4** were used with the TPP phenyl groups being replaced by H.[9] Since there was no X-ray crystal structure of **1**, we synthesized it,[6] obtained crystals by slow evaporation, and used the SHELXTL program[14] to solve its structure (see Supporting Information for structural details). We also verified that our crystals gave identical NMR spectra to those reported.[6,7]

Cu(DL-alanine)$_2$·H_2O is not the five-coordinate complex anticipated. Instead, it is a 1D polymer with water-Cu_∞ chains (d_{Cu-O} = 2.653 Å) zigzagging along the crystallographic *c*-axis (Figure 1A), and these chains are further connected by a large 3D hydrogen bond network (Figure 1B). The central unit (H_2O−Cu−H_2O) has 14 hydrogen bonds with eight neighboring Cu(DL-alanine)$_2$ and two water molecules. These structural features have dramatic effects on the hyperfine interactions, as discussed later.

The total observed chemical shift (δ_{tot}) in MAS NMR includes both a diamagnetic or orbital contribution (δ_{dia}) from paired electrons and a hyperfine contribution (δ_{hf}) from unpaired electrons.[8,9] The hyperfine shift can be further broken down into Fermi contact (δ_{FC}) and pseudocontact (δ_{pc}) terms. δ_{FC} of a given nucleus

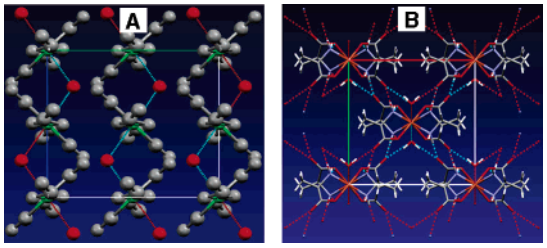

Figure 1. Unit cell of **1** viewed along (A) the *a*-axis, (water-red, Cu-green, others-gray, H omitted for clarity) and (B) the *c*-axis.

Table 1. Solid-State MAS NMR Chemical Shifts

nucleus[a]	δ^{expt} (ppm)	δ_{dia}^{calcd} (ppm)	$\rho_{\alpha\beta}$ (au)	δ_{hf}^{calcd} (ppm)	δ_{tot}^{calcd} (ppm)
1 ^{13}**C**H	−269[b]	41	−0.00323	−344	−303
1 ^{13}**C**O_2^-	−183[b]	174	−0.00400	−426	−252
1 ^{13}**C**H_3	173[b]	−6	0.00138	147	141
1 N^1**H**$_2$	−146[c]	−4	−0.00142	−168	−172
1 C^1**H**	8.4[c]	0	0.00000	0	0
1 C^1**H**$_3$	28.1[c]	−3	0.00026	31	28
4 ^{13}**C**H	86[b]	75	−0.00039	−42	33
4 ^{13}**C**H_3	−183[b]	2	−0.00151	−161	−159
4 C^1**H**	33[b]	1	0.00020	21	22
4 C^1**H**$_3$	42[b]	−3	0.00034	36	33

[a] The nucleus of interest is in bold. [b] Reference 7. T = 331 K. [c] Reference 6. T = 298 K.

depends on the spin state (S) of the system, the spin density at the nucleus ($\rho_{\alpha\beta}$), and the temperature (T):[9]

$$\delta_{FC} = m(S+1)\rho_{\alpha\beta}/T \quad (1)$$

where m is a collection of physical constants and is equal to 2.35 × 10^7 ppm K au^{-1}.[9] Usually, δ_{FC} dominates the hyperfine shift (e.g., for **1**, δ_{pc} data for ^{13}C and ^{1}H have been estimated to be from −6 to 0 ppm), and thus δ_{pc} is neglected.[8,9] Our initial DFT results for **1** using a five-coordinate Cu_1 complex resulted in large deviations from experiment (Figure 2A), but these progressively decreased with six-coordinate complexes containing 1, 3, and 9 Cu atoms (Figure 2A).[15]

As shown in Table 1 and Figure 2B, there is an excellent correlation (R^2 = 0.967) between the calculated and experimental total (chemical) shifts for **1** and **4**, with a slope of 1.007, an intercept of −21.6 ppm, and an rms error of 28 ppm or 6.3% of the whole experimental range, of 442 ppm. This almost ideal slope indicates that this functional/basis set can accurately reproduce the principal electronic interactions in the solid-state MAS NMR shifts of these paramagnetic complexes. The correlation between δ_{hf}^{calcd} and δ_{hf}^{expt} (= $\delta_{tot}^{expt} - \delta_{dia}^{calcd}$) is even better ($R^2$ = 0.980), again with an excellent slope (1.046).

In contrast to solid-state MAS NMR, single-crystal NMR/ENDOR experiments can provide accurate information on dipolar

10.1021/ja043461j CCC: $30.25

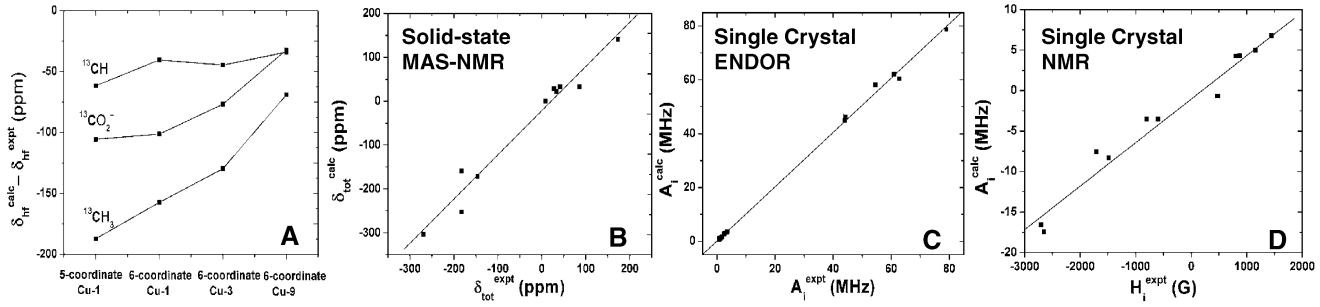

Figure 2. (A) Error of predicted hyperfine shifts in different structural models of **1**. (B) Calculated versus experimental MAS NMR total shifts for **1** and **4**. (C) Calculated versus experimental single-crystal ENDOR hyperfine data. (D) Calculated versus experimental single-crystal NMR hyperfine data.

Table 2. Single-Crystal ENDOR Hyperfine Data (in MHz)

nucleus[a]	A_1^{expt} [b]	A_2^{expt} [b]	A_3^{expt} [b]	A_1^{calcd}	A_2^{calcd}	A_3^{calcd}
2 ^{14}**N**	79.03	60.98	62.91	78.82	62.00	60.39
2 ^{1}**H**$_1$	3.57	1.73	1.15	3.59	1.62	1.13
2 ^{1}**H**$_2$	3.44	1.62	1.23	3.49	1.56	1.06
2 ^{1}**H**$_3$	3.58	1.75	1.15	3.62	1.71	1.22
2 ^{1}**H**$_4$	3.46	1.65	1.23	3.53	1.57	1.10
3 ^{14}**N**	54.47	44.26	44.07	58.30	46.31	44.97
3 ^{1}**H**$_1$	2.52	0.74	0.80	2.92	1.07	0.75
3 ^{1}**H**$_2$	2.45	0.71	0.80	2.71	0.85	0.55
3 ^{1}**H**$_3$	2.41	0.66	0.80	2.71	0.85	0.55
3 ^{1}**H**$_4$	2.49	0.69	0.80	2.92	1.07	0.75

[a] The nucleus of interest is in bold. H_{1-4} are pyrrole hydrogens. [b] Reference 4.

Table 3. Single-Crystal NMR Hyperfine Data

nucleus[a]	H_1^{expt} [b] (G)	H_2^{expt} [b] (G)	H_3^{expt} [b] (G)	A_1^{calcd} (MHz)	A_2^{calcd} (MHz)	A_3^{calcd} (MHz)
1 N^1**H**$_2$	−2706	−1485	1445	−16.58	−8.29	6.75
1 N^1**H**$_2$	−2653	−1704	1158	−17.45	−7.54	5.00
1 C^1**H**	−803	479	798	−3.56	−0.68	4.27
1 C^1**H**	−594	468	874	−3.55	−0.68	4.28

[a] The nucleus of interest is in bold. [b] Reference 2.

hyperfine couplings (T_{ii}), in addition to the Fermi contact interaction (A_{iso}). The principal components of the hyperfine coupling tensors (A_i, $i = 1, 2, 3$) are the sum of these two terms: $A_i = A_{iso} + T_{ii}$. Both A_{iso} and T_{ii} were calculated in the same manner as in our previous evaluation of EPR hyperfine data,[12] and the resulting A_i values for **1**, **2**, and **3** are given in Tables 2 and 3. These results again provide excellent predictions ($R^2 = 0.998$) for single-crystal ENDOR data, with an excellent slope (1.009) and intercept (0.10 MHz) (Figure 2C). The rms error is 0.93 MHz or only 1.2% of the entire experimental range in A_i, 78.37 MHz.

Finally, we consider the ^{1}H hyperfine shifts seen in single-crystal NMR studies of **1**. The NMR shifts (ΔH_i) are related to the hyperfine couplings A_i ($i = 1, 2, 3$) by[2,8]

$$\Delta H_i = -A_i S_c/\hbar\gamma_H \qquad (2)$$

where S_c is the Curie spin, $\hbar$ is Plank's constant divided by 2π, and γ_H is the ^{1}H gyromagnetic ratio. Since H_i^{expt} already has an S_c correction, we can plot A_i^{calcd} versus H_i^{expt}, as shown in Figure 2D. Here, we again find an excellent correlation between theory and experiment ($R^2 = 0.961$) with an intercept of −1.05 MHz (4.3% of the range of 24.20 MHz). The slope is 0.00537 MHz/G. The expected value is 0.00426 MHz/G ($\gamma_H/2\pi$).[16] The origins of the discrepancy are not certain, but since the ENDOR and MAS NMR results have <1% errors, it could be due to difficulties in accurately measuring sample temperatures (e.g., a 1 K error in T could result in 20−30% error in S_c since $T - T_c = 4.7$ K).[2]

Overall, the results presented above show that both NMR and ENDOR hyperfine properties can now be quite accurately predicted by use of DFT methods, opening up their further use in investigating paramagnetic solids, such as proteins.

Acknowledgment. This work was supported in part by the U.S. Public Health Service (NIH Grants EB-00271 and GM-50694).

Supporting Information Available: Crystal structure information for **1** and more computational details (CIF, PDF). This material is available free of charge via the Internet at http://pubs.acs.org.

References

(1) (a) La Mar, G. N. In *NMR of Paramagnetic Molecules, Principles and Applications*; La Mar, G. N., Horrocks, W. D., Jr., Holm, R. H., Eds.; Academic Press: New York, 1973; pp 86−127. (b) Walker, F. A. In *The Porphyrin Handbook*; Kadish, K. M., Smith, K. M., Guilard, R., Eds.; Academic Press: San Diego, CA, 2000; Vol. 5, pp 81−184.

(2) Sandreczki, T.; Ondercin, D.; Kreilick, R. W. *J. Am. Chem. Soc.* **1979**, *101*, 2880−2884.

(3) Sandreczki, T.; Ondercin, D.; Kreilick, R. W. *J. Phys. Chem.* **1979**, *83*, 3388−3393.

(4) Brown, T. G.; Petersen, J. L.; Lozos, G. P.; Anderson, J. R.; Hoffman, B. M. *Inorg. Chem.* **1977**, *16*, 1563−1565.

(5) Greiner, S. P.; Rowlands, D. L.; Kreilick, R. W. *J. Phys. Chem.* **1992**, *96*, 9132−9139.

(6) Liu, K.; Ryan, D.; Nakanishi, K.; McDermott, A. *J. Am. Chem. Soc.* **1995**, *117*, 6897−6906.

(7) Ishii, Y.; Wickramasinghe, N. P.; Chimon, S. *J. Am. Chem. Soc.* **2003**, *125*, 3438−3439.

(8) Wilkens, S. J.; Xia, B.; Weinhold, F.; Markley, J. L.; Westler, W. M. *J. Am. Chem. Soc.* **1998**, *120*, 4806−4814.

(9) Mao, J.; Zhang, Y.; Oldfield, E. *J. Am. Chem. Soc.* **2002**, *124*, 13911−13920.

(10) (a) Becke, A. D. *Phys. Rev. A* **1988**, *38*, 3098−3100. (b) Becke, A. D. *J. Chem. Phys.* **1993**, *98*, 5648−52.

(11) Wachters' basis (62111111/3311111/3111)for Cu and V. Wachters, A. J. H. *J. Chem. Phys.* **1970**, *52*, 1033−1036. Basis sets were obtained from the EMSL Gaussian Basis Set Order Form Web page. http://www.emsl.pnl.gov/forms/basisform.html. The DGDZVP basis for Ag, 6-311G* for other heavy atoms, and 6-31G* for hydrogen atoms are from *Gaussian 03*: Frisch, M. J., et al. *Gaussian 03*, revision B.03; Gaussian, Inc.: Pittsburgh, PA, 2003.

(12) Zhang, Y.; Gossman, W.; Oldfield, E. *J. Am. Chem. Soc.* **2003**, *125*, 16387−16396.

(13) (a) Scheidt, W. R.; Mondal, J. U.; Eigenbrot, C. W.; Adler, A.; Radonovich, L. J.; Hoard, J. L. *Inorg. Chem.* **1986**, *25*, 795−799. (b) Fleischer, E. B.; Miller, C. K.; Webb, L. E. *J. Chem. Soc.* **1964**, *86*, 2342−2347. (c) Filgueiras, C. A. L.; Horn, A., Jr.; Howie, R. A.; Skakle, J. M. S.; Wardell, J. L. *Acta Crystallogr., Sect. E* **2001**, *57*, m157−m158.

(14) *SHELXTL*, version 5.1; Bruker AXS: Madison, WI, 1998.

(15) The five-coordinate Cu-1 (Cu−H_2O), six-coordinate Cu-1 (H_2O−Cu−H_2O), six-coordinate Cu-3 (Cu−H_2O−Cu−H_2O−Cu), and the central unit (H_2O−Cu−H_2O) of the Cu-9 cluster were treated with the large basis set (see ref 11). The Cu-9 cluster includes 14 hydrogen bond partners to the central unit: a 3-21G* basis was used for the noncentral-unit atoms due to limited computational resources. This Cu-9 cluster has 1628 basis functions. For more details, see the Supporting Information.

(16) Harris, R. K. In *Encyclopedia of Nuclear Magnetic Resonance*; Grant, D. M., Harris, R. K., Eds.; Wiley & Sons: Chichester, U.K., 1996; Vol. 5.

JA043461J